INSTITUTE FOR FUSION STUDIES

DOE/ET-53088-549 IFSR #549

Vortices Associated with Toroidal Ion Temperature Gradient Driven Fluctuations

W. HORTON
Institute for Fusion Studies
The University of Texas at Austin
Austin, Texas 78712
D. JOVANOVIĆ
Institute of Physics
Yu-1101 Belgrade, Yugoslavia and
J. JUUL RASMUSSEN
Associatron EURATOM, Risø National Laboratory
Dk-4000 Roskilde, Denmark

May 1992

THE UNIVERSITY OF TEXAS

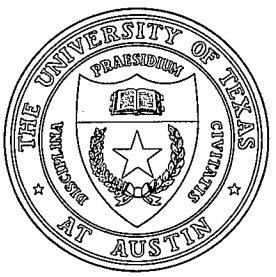

AUSTIN

Vortices Associated with Toroidal Ion Temperature Gradient Driven Fluctuations

W. Horton
Institute for Fusion Studies
The University of Texas at Austin
Austin, Texas 78712

D. Jovanović
Institute of Physics
P.O. Box 57
Yu-11001 Belgrade, Yugoslavia
and
J. Juul Rasmussen
Associatron EURATOM, Risø National Laboratory
P.O. Box 49
Dk-4000 Roskilde, Denmark

Abstract

The three nonlinear hydrodynamic equations for potential, parallel ion velocity and ion pressure used in simulations of the toroidal ion temperature gradient driven fluctuations and transport in a shear magnetic field are analyzed for coherent vortex structures. Two types of vortex structures are found: one type for weak shear that is a generalization of the usual modon vortex construction and the second type of solution for strong magnetic shear where the convective nonlinearity in the parallel velocity field generates a cubic trapping nonlinearity in the vorticity equation. These vortex structures show the possibility of explaining the saturated states observed in the numerical simulations as self-organized nonlinear states in contrast to wave turbulence.

PACS Nos. are: 03.40.Kf, 52.25.Fi, 52.35.Kt, and 52.35.Mw

I. Introduction

The ion temperature gradient driven drift wave turbulence is an important mechanism for the transport of ion thermal energy across a confining magnetic field. The linear instability and the early nonlinear stages of the turbulent fluctuations have been extensively studied both in early simulations and more recently in Refs. 1–4. The simulations such as Hong and Horton,[2] with both magnetic shear and the local unfavorable magnetic field curvature and gradient, show that in the late stages of nonlinear evolution larger scale coherent structures are formed. In this stage there is a partial alignment of the fluctuations of the hydrodynamic fields due to the relatively fast $\mathbf{E} \times \mathbf{B}$ convection of the plasma around the local minima and maxima of the electrostatic potential.

As a result of the coherent vortical structures induced by the local $\mathbf{E} \times \mathbf{B}$ rotations there is a reduction of the radial transport (due to the trapping in the vortex cores) from the cross-field transport rate found in the early stage of saturation. Thus it is important to understand the nature of these coherent structures in the presence of both magnetic shear and $\mathbf{E} \times \mathbf{B}$ shear flows.

In the present work we investigate the conditions forced on the fluctuation fields in hydrodynamic descriptions for the formation of coherent structures propagating in the magnetic surfaces. The conditions lead to nonlinear elliptic equations with spatially varying coefficients describing the nonuniformity in the equilibrium induced by the magnetic shear and the sheared flows. Earlier studies by Su *et al.*[5] for the sub-case of vanishing ion pressure shows the possibility of long-lived coherent vortices in the presence of magnetic shear. Here, we look for such solutions analytically and numerically in the more interesting case of a system which contains the driving force for linear instability. With the addition of the third dynamical equation describing the ion pressure fluctuations the linear dynamics is described by a third

order polynomial in the complex frequency ω and one root is unstable for $\eta_i > \eta_{crit} \simeq \Gamma - 1$ where η_i is the ratio of the ion temperature gradient to the density gradient and Γ is adiabatic constant describing compressibility in the ion thermal balance equation. The details of the linear stability conditions and the early stages of the nonlinear dynamics are given in Refs. 1–4. Three-dimensional nonlinear simulations showing the saturated state of turbulent vortical convection are found in Refs. 6 and 7. Two-dimensional toroidal η_i-mode simulations in a periodic box without parallel mass flow ($v_{||} = 0$) are shown by Ottaviani *et al.*[8] to give rise to large scale ($\gtrsim 10\rho_s$) vortices with radial transport reduced from the quasilinear value.

II. Model Equations

We study the nonlinear regime of the toroidal η_i-mode in a collisionless plasma, which has the inhomogeneous density $n_0(x)$, and ion temperature $T_i(x)$:

$$\begin{aligned} n_0(x) &= n_0 \left(1 - \frac{x - x_0}{L_n}\right) \\ T_i(x) &= T_{i0} \left(1 - \frac{x - x_0}{L_T}\right) \end{aligned} \tag{1}$$

where $\eta_i = L_n/L_T$. The plasma is confined in a torus whose major radius is R, and immersed in a sheared magnetic field $B_0(x)\mathbf{e}_{||}$. The toroidicity is defined by the parameter $\varepsilon_n = L_n/R$, and the magnetic shear by the shear length L_s where in local x, y, z coordinates the magnetic field may be written as

$$B_0(x) = B_0 \left(1 - \frac{x}{R}\right) \tag{2a}$$

$$\mathbf{e}_{||} = \mathbf{e}_z + \frac{x - x_0}{L_s}\,\mathbf{e}_y - \frac{z - z_0}{R}\,\mathbf{e}_x \,.$$

There also exists a macroscopic sheared flow, both in the parallel and perpendicular direction, whose fluid velocity is $\mathbf{V}_0(x)$:

$$\mathbf{V}_0(x) = c_s \left[\left(\frac{x - x_0}{L_{||}}\right)\mathbf{e}_z + \left(\frac{x - x_0}{L_\perp}\right)\mathbf{e}_y\right] \tag{2b}$$

where $c_s = (T_e/m_i)^{1/2}$ is the ion sound speed. For drift-wave-type perturbations, with the characteristic phase velocity in the parallel direction being much smaller than the electron thermal speed, electrons are Boltzman distributed,

$$n_e \simeq n_0(x)\left(1+\frac{e\phi}{T_e}\right) , \tag{3}$$

and we can neglect the inhomogeneity of the electron temperature T_e.

A closed system of equations, describing the plasma state in terms of the electrostatic potential ϕ, parallel ion velocity $v_{\|i}$, and the ion pressure p_i can be obtained from the ion hydrodynamics.[1] The derivation of the reduced drift wave equation[1] assumes $\rho_s/L \ll \rho_s \nabla_\perp \ll 1$ where $\rho_s = (m_i T_{e0})^{1/2}/e B_0$ is the ion inertial scale length and L is some typical scale length. To the leading order in small parameters ρ_s/L, making use of quasineutrality and the electron Boltzmann distribution, Eq. (3) (i.e. assuming zero electron mass) the equations of ion continuity, parallel momentum, and energy, can be written as[1-7]:

$$\left(\frac{\partial}{\partial t}+\mathbf{V}_\perp\cdot\nabla\right)\left[(1-\nabla_\perp^2)\Phi - x\right] + \partial_\| V_\|$$

$$= (\mathbf{e}_z\times\nabla)\cdot\{[(\mathbf{e}_z\times\nabla P)\cdot\nabla]\,\mathbf{V}_\perp\} + 2\varepsilon_n\frac{\partial}{\partial y}(P+\Phi) \tag{4}$$

$$\left(\frac{\partial}{\partial t}+\mathbf{V}_\perp\cdot\nabla\right) V_\| = -\partial_\|(P+\Phi) \tag{5}$$

$$\left(\frac{\partial}{\partial t}+\mathbf{V}_\perp\cdot\nabla\right) P + \Gamma\partial_\| V_\| = 2\Gamma\varepsilon_n\frac{\partial}{\partial y}\left[\left(1-\frac{T_{i0}}{T_e}-\frac{K}{2\varepsilon_n}\nabla_\perp^2\right)\Phi + 2P\right] . \tag{6}$$

Here the standard dimensionless drift wave variables are used:

$$\begin{aligned} &x\to\frac{x-x_0}{\rho_s}\,, \quad y\to\frac{y}{\rho_s}\,, \quad z\to\frac{z-z_0}{L_n}\,, \quad t\to\frac{tc_s}{L_n}\,, \\ &\Phi=\frac{e\phi}{T_e}\frac{L_n}{\rho_s}\,, \quad V_\| = \frac{v_{\|i}}{c_s}\frac{L_n}{\rho_s}\,, \quad P=\frac{p_i}{n_0 T_e}\frac{L_n}{\rho_s} \end{aligned} \tag{7}$$

Besides that, the velocity $\mathbf{V}_\perp$ in Eqs. (4)–(6) denotes the perpendicular component of the ion guiding center velocity, which is the sum of the macroscopic shear flow, and the $\mathbf{E}\times\mathbf{B}$

drift

$$\mathbf{V}_\perp = S_\perp x\, \mathbf{e}_y + \mathbf{e}_z \times \nabla\Phi = \mathbf{e}_z \times \nabla \left(\Phi + S_\perp \frac{x^2}{2} \right) . \tag{8}$$

It is convenient also to express the dimensionless parallel ion velocity $V_\parallel$, and pressure P as the sum of the corresponding zero order and perturbed quantities

$$\begin{aligned} V_\parallel &= S_\parallel x + v \\ P &= -Kx + p \, . \end{aligned} \tag{9}$$

Finally, $\partial_\parallel$ denotes derivative in the direction parallel to the magnetic field

$$\partial_\parallel = \frac{\partial}{\partial z} + S_m x \frac{\partial}{\partial y} . \tag{10}$$

The following standard notation is used in the above equations (4)–(10):

$$\begin{aligned} &S_\perp = \frac{L_n}{L_\perp}, \quad S_\parallel = \frac{L_n}{L_\parallel}, \quad S_m = \frac{L_n}{L_s}, \quad \varepsilon_n = \frac{L_n}{R} \\ &\eta_i = \frac{L_n}{L_T}, \quad K = \frac{T_{i0}}{T_e}(1+\eta_i), \quad \Gamma = \gamma \frac{T_{i0}}{T_e} \end{aligned} \tag{11}$$

where $\gamma = C_p/C_v$ is the ratio of the plasma specific heats, which for a collisionless fluid may be taken as variable $1 < \gamma < 3$ in order to match the description from the Vlasov equation.

Equations (4)–(6) account for all the relevant finite ion Larmor radius, toroidicity, and shear related effects. Thus, the first term on the right-hand side of the ion continuity equation (4) represents the combination of the convection by the diamagnetic drift, and the finite Larmor radius nonlinearities (note that a cancellation between the finite Larmor radius (FLR) terms, and a part of the diamagnetic drift convective nonlinearities occurs), while the second term arises from the convection by the ion toroidal drift. The right-hand side of the energy equation (6) describes the compressibility from cross-field transport.

The linear dispersion relation which is obtained from Eqs. (4)–(6) reveals the existence of an unstable mode $\omega_k + i\gamma_k$ driven by the ion temperature gradient. The mode has two limiting forms depending on the ratio $k_\parallel c_s$ to $\omega_D = 2\varepsilon_n \omega_*$. One limit is existing in the slab geometry[6,7,9] ($k_\parallel c_s \gg \omega_D$), where the coupling is achieved by the parallel ion motion along

the sheared field line, and the unstable mode is essentially an ion acoustic wave in which the restoring force $k_{||}(\Phi + p_i) = k_{||}(1 - \omega_{*pi}/\omega)\Phi$ becomes negative due to the dominance of the convection of the pressure for $\omega_{*pi}/\omega > 1$. The other limit, which exists when the toroidal effects dominate,[8,10] is of the interchange nature, and for tokamak systems, this branch typically has a larger growth rate than the ion acoustic branch.

III. Stationary Solution

Equations (4)–(6) belong to a class of nonlinear partial differential equations with vector product (or Poisson bracket) type nonlinearities, and one may expect that they possess a localized solution in the form of a travelling double vortex. In the shearless case, such a vortex solution has been constructed in the simple cases of absence of toroidal effects[11] and parallel ion motion.[12] The authors of Ref. 3 attempted to study the effects of shear on such coherent structures, in the case of strictly two-dimensional ions, $\frac{\partial}{\partial z} = 0$. They include the curvature related terms in the ion continuity (4), but neglect similar terms in the thermal balance equation (6). Furthermore, they also neglect finite Larmor radius and diamagnetic drift nonlinearities in Eq. (4) (the first term on the right-hand side).

In this section we construct a double vortex solution of the complete system of equations (4)–(6), in the low ion temperature regime $T_i \ll T_e$. We seek a solution which is stationary and z-independent in the reference frame moving with the velocity:

$$\mathbf{V}_{ph} = u(\mathbf{e}_y + \alpha^{-1}\mathbf{e}_z) \,, \tag{12}$$

i.e. we assume all perturbed quantities to be dependent only on x and $y' = y + \alpha z - ut$. Then we can readily rewrite the convective and parallel derivatives as

$$\frac{\partial}{\partial t} + \mathbf{V}_\perp \cdot \nabla = \left[\mathbf{e}_z \times \nabla \left(\Phi - ux + S_\perp \frac{x^2}{2}\right)\right] \cdot \nabla$$

$$\partial_{||} = \left[\mathbf{e}_x \times \nabla \left(\alpha x + S_m \frac{x^2}{2}\right)\right] \cdot \nabla \tag{13}$$

and

$$\frac{\partial}{\partial y} = (\mathbf{e}_z \times \nabla x) \cdot \nabla \ .$$

Here α determines the pitch of the structure that becomes a helical structure when y is periodic with $y = r\theta$. If we also assume low ion temperature, and weak shear:

$$\begin{aligned} \Gamma\alpha \sim \Gamma\,\varepsilon_n \ll 1 \\ \max(S_m, S_\perp, S_\parallel) \equiv S \ll 1 \end{aligned} \tag{14}$$

we may treat the right-hand side of the energy equation (6) as a small perturbation. First, we set $\Gamma = 0$, and Eq. (6) readily obtains the simple form of a Poisson bracket, when it can be integrated to yield

$$\Phi - ux + S_\perp \frac{x^2}{2} = F \tag{15}$$

where $F = F(p - Kx)$ is an arbitrary function of its argument. Substituting solution (15) into Eqs. (5) and (4), we can integrate them in the same way:

$$v + S_\parallel x - \left(1 + \frac{1}{F'}\right)\left(\alpha x + S_m \frac{x^2}{2}\right) = G \tag{16}$$

$$F'\left[-\nabla^2 F + (2\varepsilon_n - 1 + u)x - S_\perp \frac{x^2}{2}\right] + 2\varepsilon_n x + \frac{F''}{2F'^2}\left(\alpha x + S_m \frac{x^2}{2}\right)^2$$

$$-G'\left(\alpha x + S_m \frac{x^2}{2}\right) - \nabla_\perp^2 F + \frac{F''}{2}[\nabla(p - Kx)]^2 = H \ . \tag{17}$$

Here $G = G(p - Kx)$, $H = H(p - Kx)$ are also arbitrary functions, and $F^{(n)}, G^{(n)}, H^{(n)}$ denote n-th derivatives of these functions. In the derivation of Eq. (17) we used the following identities:

$$\nabla\left\{[(\mathbf{e}_z \times \nabla\xi) \cdot \nabla]\nabla F(\xi)\right\} = (\mathbf{e}_z \times \nabla\xi) \cdot \nabla\left[\nabla^2 F(\xi) + F''(\xi) \cdot \frac{1}{2}(\nabla\xi)^2\right]$$

$$(1 - \nabla^2)\Phi = F(p - Kx) - \nabla^2 F(p - Kx) + ux - S_\perp \frac{x^2}{2} + S_\perp \ . \tag{18}$$

Note that Eqs. (15)–(17) are valid for arbitrary values of the shear coefficients $S_m, S_\perp, S_\parallel$, provided the effects of the compressibility are negligible, $\Gamma = 0$.

In the shearless case,[11,12] the standard double vortex is constructed by adopting linear functions F, G, H, and allowing them to have different slopes inside and outside of the circular vortex core. In the presence of weak shear,[3] however, a similar solution is possible if these functions have small nonlinear parts:

$$\frac{F''}{F'} \sim \frac{G''}{G'} \sim \frac{H''}{H'} \sim \max(S_m, S_\perp, S_\parallel) \ll 1 \ . \tag{19}$$

As the first order correction to the "cold" solution (15)–(17), we include thermal terms in the energy equation using the "cold" expressions for $v, \Phi, \nabla^2\Phi$

$$\partial_\parallel V_\parallel = \left[\mathbf{e}_z \times \nabla \left(\alpha x + S_m \frac{x^2}{2}\right)\right] \cdot \nabla \left[-S_\parallel x + \left(1 + \frac{1}{F'}\right)\left(\alpha x + S_m \frac{x^2}{2}\right) + G\right]$$

$$\frac{\partial}{\partial y}\left[\left(1 - \frac{T_{i0}}{T_e} - \frac{K}{2\varepsilon_n}\nabla^2\right)\Phi + 2P\right] = (\mathbf{e}_z \times \nabla x) \cdot \left[\left(1 - \frac{T_{i0}}{T_e}\right)F + \frac{K}{2\varepsilon_n}\frac{H}{1+F'} + 2(p - Kx)\right] \tag{20}$$

which permits us to rewrite the thermal balance equation in the form of a complete Poisson bracket, and to solve it as:

$$\Phi - ux + S_\perp \frac{x^2}{2} = F\left[p - (K + \delta K)x\right] \ . \tag{21}$$

Here F is the same function as the one defined in Eq. (15), with a slightly perturbed argument

$$\delta K = -2\Gamma\,\varepsilon_n \left[1 - \frac{T_{i0}}{T_e} + \frac{1}{F'}\left(2 - \frac{\alpha}{\varepsilon_n}G' + \frac{K}{\varepsilon_n}\frac{H'}{1+F'}\right)\right] \ , \tag{22}$$

where only leading order expressions for F', G', H' are used. Similarly, substituting Eq. (21) into the ion parallel momentum, and continuity equations, and after a somewhat lengthy but straightforward algebra, we completely recover Eqs. (16) and (17), but with a small perturbation of the arguments of the functions G and H:

$$G = G\left[p - (K + \delta K)x\right] \tag{23}$$

$$H = H\left[p - \left(K + \frac{F'}{1+F'}\delta K\right)x\right] \ . \tag{24}$$

Asymptotic expressions for the functions F, G, H, in the limit of large arguments ($x \to \infty$) are obtained from the condition that the perturbations of the ion velocity v, pressure p, and potential Φ vanish for $x \to \infty$. Substituting $v = p = \Phi = 0$ in Eqs. (15)–(17), (21), (22)–(24) we obtain the following asymptotic expressions:

$$F(\xi) = F_1 \cdot \xi + F_2 \cdot \xi^2 \tag{25}$$

$$G(\xi) = G_1 \cdot \xi + G_2(\xi) \cdot \xi^2 \tag{26}$$

$$H^{\text{out}}(\xi) = H_1^{\text{out}} \cdot \xi + H_2^{\text{out}}(\xi) \cdot \xi^2 \tag{27}$$

where the coefficients $F_i, G_i, H_i^{\text{out}}$ are given by:

$$\begin{aligned}
F_1 &= \frac{u}{K + \delta K} \\
F_2 &= \frac{S_\perp}{2K^2} \\
G_1 &= \frac{-S_\parallel}{K + \delta K} + \alpha \left(\frac{1}{u} + \frac{1}{K + \delta K} \right) \\
G_2(\xi) &= \frac{-1}{2K^2(F_1 + 2F_2\xi)} \left[S_m(1 + F_1 + 2F_2\xi) + 2S_\perp \frac{\alpha}{u} \right] \\
H_1^{\text{out}} &= \frac{-1}{K + \delta K} \cdot [(1 + F_1) \cdot 2\varepsilon_n - F_1(1 - u) - G_1\alpha] \\
H_2^{\text{out}}(\xi) &= \frac{1}{2K^2} \Bigg[- F_1 S_\perp - G_1 S_m - 4K F_2(2\varepsilon_n - 1 + u) \\
&\qquad + \frac{2F_2}{(F_1 + 2F_2\xi)^2} + 4K\alpha G_2(\xi) \Bigg]
\end{aligned} \tag{28}$$

and we dropped all small terms of the order $S\Gamma$, S^2, and higher.

The shear induced vortex equations of Su *et al.*[5] are recovered when $\alpha = S_\perp = S_\parallel = 0$ and K is sufficiently small. In this limit Eqs. (15), (16) and (25)–(27) give the $v(x, y)$ in Eq. (17)

of Su *et al.*[5] In Sec. IV we will derive the corresponding shear induced vortex structure that follows in this strong shear limit.

In the standard vortex scenario, spatially localized solutions of Eqs. (15)–(17) are constructed by adopting different analytic expressions for the functions F, G, H in two different regions of the x-y-plane, outside and inside the vortex core. Obviously, in such a case the functions F, G, H must be constant along the core edge. However, the arguments of F and G differ from the argument of H, see Eqs. (22)–(24), and there can not exist any common closed equiline for all three functions. Consequently, if we allow for only one closed line of discontinuity, some of the functions F, G, H must have the same analytic form on the whole x-y plane, both inside and outside the vortex core.

We adopt functions F, G in the form (25), (26) on the whole x-y plane, while the asymptotic form of H, Eq. (27) is taken to be valid only in the exterior region. If the vortex radial scale r_0 is much smaller than the shear length, $Sr_0 \ll K$, with the same accuracy as above, we may adopt within the core a weakly nonlinear function H:

$$H^{\rm in}(\xi) = H_0^{\rm in} + H_1^{\rm in}\xi + H_2^{\rm in}\xi^2 \tag{29}$$

where the constants $H_0^{\rm in}, H_1^{\rm in}, H_2^{\rm in}$ satisfy $H_1^{\rm in} \gg H_0^{\rm in}, H_2^{\rm in}$.

The approximative solution of Eqs. (15)–(17), which is valid only at distances which are much shorter than the shear length, is obtained after linearization around $p - Kx = 0$. The first order problem and its solution, as one may have expected from the Hasegawa-Mima equation, is given by

$$\begin{aligned} &(\nabla^2 - \rho^2)p_1 = 0\ , && r = (x^2+y^2)^{1/2} > r_0 \\ &(\nabla^2 + \kappa^2)(p_1 - wx) = 0\ , && r < r_0 \end{aligned} \tag{30}$$

where, in the usual way, we adopted the vortex core to be a circle with the radius r_0, and:

$$\rho^2 = \frac{-H_1^{\rm out}}{F_1(1+F_1)} = \frac{u-1}{u+K+\delta K} + \frac{2\varepsilon_n}{u} + \frac{\alpha S_{\|}}{u(u+K)} - \frac{\alpha^2}{u^2}$$

$$\kappa^2 = \frac{H_1^{\rm in}}{F_1(1+F_1)}$$

$$w = \left(K + \delta K \cdot \frac{u}{u+K}\right) \cdot \frac{\kappa^2+\rho^2}{\kappa^2} \ . \tag{31}$$

Linear solution has the usual dipole vortex (or modon) form:

$$p_1 = r_0 \cos\theta \cdot \left(K + \delta K \cdot \frac{u}{u+K}\right) \begin{cases} \left(1+\frac{\rho^2}{\kappa^2}\right)\frac{r}{r_0} - \frac{\rho^2}{\kappa^2}\frac{J_1(\kappa r)}{J_1(\kappa r_0)} \ , & r < r_0 \\ \frac{K_1(\rho r)}{K_1(\rho r_0)} \ , & r > r_0 \end{cases} \tag{32}$$

where J_1, K_1 are ordinary, and modified Bessel functions of the first order, and $\theta = \mathrm{arctg}\,\frac{y}{x}$. Wavenumber κ (or, equivalently, the slope $H_1^{\rm in}$) is found from the continuity of $\frac{\partial}{\partial r_0} p_1(r_0)$, yielding the following nonlinear dispersion relation:

$$\frac{-1}{\kappa}\frac{J_2(\kappa r_0)}{J_1(\kappa r_0)} = \frac{1}{\rho}\frac{K_2(\rho r_0)}{K_1(\rho r_0)} \ . \tag{33}$$

The first order correction δp is found after linearization around $p_1 - Kx$, yielding a driven Hasegawa-Mima equation:

$$\begin{aligned} (\nabla_\perp^2 - \rho^2)\delta p &= \mathcal{P} \ , \quad r > r_0 \\ (\nabla_\perp^2 + \kappa^2)\delta p &= \mathcal{P} \ , \quad r < r_0 \end{aligned} \tag{34}$$

where the driving term $\mathcal{P}$ is built by the first order modon p_1:

$$\mathcal{P} = \frac{-1}{F_1(1+F_1)} \cdot \left\{ \left(\frac{1}{2}+F_1\right) \cdot F_2 \left[\nabla^2(p_1 - Kx)^2 + 2(p_1 - Kx)\nabla^2 p_1\right] \right.$$

$$\left. + H_2(p_1 - Kx)^2 - g_1 x(p_1 - Kx) - g_2\, x^2 + H_0^{\rm in} h(r - r_0) \right\}$$

$$\begin{aligned} g_1 &= 2\left[F_2 \cdot (2\varepsilon_n - 1 + u) - \alpha\, G_2(0)\right] \\ g_2 &= \frac{1}{2}\left[F_1\, S_\perp + G_1\, S_\perp + \frac{2F_2\,\alpha^2}{F_1^2}\right] \ . \end{aligned} \tag{35}$$

Here $h(r-r_0)$ is the Heaviside unit step function, and H_2 denotes $H_2^{\rm out}(0)$, $H_2^{\rm in}$, respectively.

Noting that the first order solution p_1 contains only the first cylindrical harmonic, the driving term $\mathcal{P}$ and consequently also the second order solution δp, will have only cylindrically symmetric (monopole), and quadrupole parts:

$$\begin{aligned} \mathcal{P} &= \mathcal{P}_0(r) + \mathcal{P}_2(r)\cos 2\theta \\ \delta p &= \delta p_0(r) + \delta p_2(r)\cos 2\theta \ . \end{aligned} \tag{36}$$

Equation (34) can be easily integrated using the Cauchy method of variation of constants, yielding:

$$\delta p_n(r) = \begin{cases} J_n(\kappa r)\cdot[a_n + \mathcal{Y}_n(r)] + Y_n(\kappa r)\mathcal{J}_n(r) \ , & r < r_0 \\ K_n(\rho r)\,[b_n + \mathcal{I}_n(r)] + I_n(\rho r)\mathcal{K}_n(r) \ , & r > r_0 \ , \quad n = 0, 2 \end{cases} \tag{37}$$

where J_n, Y_n and I_n, K_n are ordinary, and modified Bessel functions of the n-th order, a_n, b_n are constants of integration, and:

$$\mathcal{Y}_n(r) = -\frac{\pi}{2}\int_{r_0}^{r} dr' r'\, Y_n(\kappa r')\mathcal{P}_n(r') \tag{38}$$

$$\mathcal{J}_n(r) = \frac{\pi}{2}\int_{0}^{r} dr' r'\, J_n(\kappa r')\mathcal{P}_n(r') \tag{39}$$

$$\mathcal{I}_n(r) = -\int_{r_0}^{r} dr' r'\, I_n(\rho r')\mathcal{P}_n(r') \tag{40}$$

$$\mathcal{K}_n(r) = \int_{\infty}^{r} dr' r' K_n(\rho r')\mathcal{P}_n(r') \ , \quad n = 0, 2 \ . \tag{41}$$

Solution (37) is finite at $r = 0, \infty$, and the continuity of δp at $r = r_0$ yields:

$$\begin{aligned} a_n &= \frac{1}{J_n(\kappa r_0)}\,[\delta p_n(r_0) - Y_n(\kappa r_0)\mathcal{J}_n(r_0)] \\ b_n &= \frac{1}{K_n(\rho r_0)}\,[\delta p_n(r_0) - I_n(\rho r_0)\mathcal{K}_n(r_0)] \ , \quad n = 0, 2 \ . \end{aligned} \tag{42}$$

As we have adopted the circular vortex core with the radius r_0, to be centered at $x = 0, y = 0$, continuity of the function H yields:

$$\begin{aligned} \delta p_0(r_0) &= \frac{H_0^{\text{in}}}{H_1^{\text{out}} - H_1^{\text{in}}} \\ \delta p_2(r_0) &= 0 \ . \end{aligned} \tag{43}$$

Finally, from the continuity of $\nabla\delta p$ at $r = r_0$, which for our choice of the vortex core corresponds to the continuity of $\frac{\partial}{\partial r_0}\delta p_n(r_0), n = 0, 2$, we obtain the following equations from which the remaining constants of integration $H_0^{\rm in}, H_2^{\rm in}$ can be determined:

$$\frac{\mathcal{K}_0(r_0)}{K_0(\rho r_0)} - \frac{\pi}{2}\frac{\mathcal{J}_0(r_0)}{J_0(\kappa r_0)} = \delta p_0(r_0)\cdot\left[\frac{\rho K_1(\rho r_0)}{K_0(\rho r_0)} - \frac{\kappa J_1(\kappa r_0)}{J_0(\kappa r_0)}\right] \tag{44}$$

$$\frac{\mathcal{K}_2(r_0)}{K_2(\rho r_0)} - \frac{\pi}{2}\frac{\mathcal{J}_2(r_0)}{J_2(\kappa r_0)} = 0\ . \tag{45}$$

Far from the modon core the shear-related terms can not be considered any longer as being small. In this "far away" region, behavior of the vortex is described essentially by linear equations. Linearizing Eqs. (15)–(17) around $p = 0$, we obtain for the first order solution p_1:

$$-(1 + F_1 - 2F_2Kx)\cdot(F_1 - 2F_2Kx)\nabla^2 p_1 + \left(\frac{1}{2} + F_1 - 2F_2Kx\right)\cdot 4F_2K\frac{\partial p_1}{\partial x}$$

$$-\left(H_1^{\rm out} - 2Kx H_2^{\rm out}(-Kx)\right)p_1 = 0\ . \tag{46}$$

One may observe the existence of a turning layer $x = x_t$ in Eq. (46), defined by $H_1^{\rm out} = 2Kx_tH_2^{\rm out}(-Kx_t)$, where the coupling of vortices with linear drift waves takes place. Furthermore, there are two resonant layers $x = x_1, x_2$ given by $F_1 = 2F_2Kx_1$, and $1 + F_1 = 2F_2Kx_2$, or equivalently:

$$\begin{aligned} u &= S_\perp x_1 \\ u &= K + \delta K + S_\perp x_2\ . \end{aligned} \tag{47}$$

In these resonant layers we have $\Phi = 0$, and $\Phi + p = 0$, respectively, and the resonance occurs due to the perpendicular shear flow.

Due to the existence of the singular layers introduced by $S_\perp \neq 0$ the vortex formation is expected to proceed in the manner shown in Horton *et al.*[13] and Tajima *et al.*[14] where the drift wave-Kelvin Helmholtz vortices are investigated analytically and numerically. On the other hand the turning point layer $x = x_t$ introduces the physics of oscillatory tails on one side of the vortex structure. Thus, a thorough solution of the vortex structure problem with

both the K and $S_\perp$ effects of order unity awaits further numerical analysis. The contours of Φ in such a regime will be complicated. An indication of the structure is given by the results of the 3D simulation in Ref. 15 with $K = 3, \Gamma = 2, S_m = 0.3$ and $L_s v'_E/c_s = 1.5$ showing vortices that are stretched in the y direction.

IV. Strong Magnetic Shear Induced Dipoles

Now we consider the regime where the magnetic shear S_m is sufficiently strong to produce nonlinear binding into a vortex structure through the $\mathbf{E} \times \mathbf{B}$ convection in the ion-acoustic waves. The $\mathbf{E} \times \mathbf{B}$ convection of the parallel ion velocity produces the nonlinearity $G(\xi) = G_1\xi + G_2\xi^2$ in Eq. (16) and this quadratic nonlinearity couples into the vorticity Eq. (17) to produce a cubic trapping potential proportional to $S_m^2\Phi^3$. In this strong shear limit we generalize the results of Su *et al.*[5] to the case of the ion temperature gradient driven fluctuations.

To proceed analytically we take the limit $S_\perp = 0$ and neglect the effect of compressibility, $\Gamma = 0$. With these simplifications we obtain for G_1 and G_2

$$G_1 = -\frac{S_\parallel}{K} + \frac{\alpha}{K}\left(1 + \frac{K}{u}\right) \qquad G_2 = -\frac{S_m}{2K^2}\left(1 + \frac{K}{u}\right) \tag{48}$$

with the associated parallel velocity given by

$$v = \left[\frac{S_m x^2}{2} - \frac{S_m}{2K^2}(p - Kx)^2\right]\left(1 + \frac{K}{u}\right) . \tag{49}$$

Using these results for $G(\xi)$ in the equation for $H(\xi)$,

$$H(\xi) = H_1\xi + H_2\xi^2 + H_3\xi^3 \tag{50}$$

we derive that

$$H_1 = \frac{u}{K^2}(u - 1 - 2\varepsilon_n) - \frac{2\varepsilon_n}{K} + \frac{\alpha G_1}{K}$$

$$H_2 = -\frac{S_m G_1}{2K^2} + \frac{2\alpha}{K} G_2$$

$$H_3 = -\frac{S_m G_2}{K^2} \ . \tag{51}$$

Thus, we see that the cubic nonlinearity in the vorticity equation arises from the G_2 which in turn arises from the convective nonlinearity in the parallel velocity equation. Substituting these results for $H(\xi)$ into Eq. (17) we obtain the cubic vortex equation for $p(x, y')$, where $y' = y + \alpha z - ut$, given by

$$\begin{aligned} &\nabla^2 p - \left(\frac{u-1}{u+K} + \frac{2\varepsilon_n}{u} + \frac{\alpha S_{||}}{u(u+K)} - \frac{\alpha^2}{u^2} \right) p \\ &= \frac{S_m}{2uK} \left(\frac{\alpha}{u} - \frac{S_{||}}{u+K} \right) p^2 - \frac{S_m x}{u} \left(\frac{2\alpha}{u} - \frac{S_{||}}{u+K} \right) p \\ &- \frac{S_m^2}{2u^2 K^2} \left(p^3 - 3Kxp^2 + 2K^2 x^2 p \right) \ . \end{aligned} \tag{52}$$

Equation (52) has the symmetry property that if $p(x, y)$ is a solution then $-p(-x, y)$ is also a solution. Thus, we may take the natural modes as having dipole symmetry. Secondly we see that for such an odd (in x) solution the nonlinearity dominates the core region when $p(x, 0) = x(dp/dx)_0 > Kx$ which is equivalent to the statement that pressure fluctuation in the core exceeds the equilibrium (ambient) pressure gradient. In terms of the potential Φ the corresponding relation is that the v_y-flow in the core of the vortex rest frame is reversed so that $d\Phi/dx > u$. Solving Eq. (52) with $|p| \to 0$ as $|x| \to \infty$ leads the nonlinear eigenvalue problem.

Let us consider a reduced form of Eq. (52) where the ion temperature gradient parameter K and the toroidicity $2\varepsilon_n$ are retained and look for the solutions centered on the rational surface at $x = 0$ with $\alpha = S_{||} = 0$. Introducing the function $\psi = p/K = \Phi/u$ we can rewrite the equation in the form

$$\nabla^2 \psi = -\frac{\partial V_{\text{eff}}}{\partial \psi} (\psi, x) \tag{53}$$

with

$$V_{\text{eff}}(\psi, x) = -\frac{1}{2} \left[k^2(u) - \frac{S_m^2 x^2}{u^2} \right] \psi^2 + \frac{S_m^2 x}{2u^2} \psi^3 + \frac{S_m^2 \psi^4}{8u^2}$$

$$k^2(u) = \frac{u-1}{u+K} + \frac{2\varepsilon_n}{u} \tag{54}$$

and $k^2(u)$ equals the characteristic e-folding number ρ^2, Eq. (31), in the limit $\Gamma = \alpha = S_\perp = S_\parallel = 0$. Equation (53) clearly shows the trapping nature of the nonlinear potential due to the positive definite term $S_m^2\psi^4/u^2$.

To study the trapping of the fluctuation in x we consider the variation in x along $y = 0$ with the approximation that $\partial^2\psi/\partial y^2 = -\psi(x,0)/b^2$ which shifts $k^2(u) \to k^2(u) + 1/b^2$. (In the future full 2D solutions should be available.) Without the x-dependence the soliton-like solution occurs along the homoclinic orbits of $\partial^2\psi/\partial x^2 = -\partial V_{\text{eff}}/\partial\psi$ which are defined by

$$\left(\frac{d\psi}{dx}\right)^2 = k^2\psi^2 - \frac{S_m^2}{8u^2}\psi^4 \,. \tag{55}$$

In the presence of the x-dependence the nonlinear eigenfunction starts outside the separatrix and comes into the small amplitude ($\psi^2 \to 0$) external region along the stable manifolds given by $d\psi/dx = \pm k\psi$.

In Fig. 1 we show the "trajectory" of the solution in the phase space $(\psi, d\psi/dx)$ and in Fig. 2a the localized vortex (nonlinear) eigenfunction. The three components of the energy density are shown in Fig. 2b. The energy densities are the electrostatic energy in the adiabatic electron distribution Φ^2, the kinetic energy in the $\mathbf{E}\times\mathbf{B}$ circulation of the ions $(\nabla\Phi)^2$, and the kinetic energy in the parallel oscillations of the ions given by v^2 from Eq. (49) (reduced to $\alpha = S_\parallel = 0$). The figure shows that very little fluctuation energy escapes beyond $x = \Delta x/\rho_s \cong 5$. In the figures the dimensionless $s = S_m/ku^2 = 1/4$. For stronger magnetic shear S_m, although the binding is stronger, the coupling to the exterior ion acoustic waves increases raising the tail energy density visible in Fig. 2b.

The maximum of the vortex potential occurs near the separatrix as seen from Fig. 1, for the example, which from Eq. (55) gives

$$\Phi_{\max} = u\psi_{\max} = \frac{2\sqrt{2}\,u^2|k(u)|}{|S_m|} \tag{56}$$

where $k(u) = [(u-1)/(u+k) + 2\varepsilon_n/u + 1/b^2]^{1/2}$. The condition $k^2(u) > 0$ is the generalization of the usual condition that the velocity u of the vortex must lie outside (but may be very close to the boundary) of the region of linear wave propagation which is defined by $k^2(u = \omega/k_y, b = k_y^2) \leq 0$. Thus, for vortices with velocities u just outside the linearly unstable domain of the ion temperature gradient instability there exists nonlinear vortex fluctuation states. We believe that the coherent vortex states computed here are idealized models for the vortices seen in the simulations of Refs. 2 and 7.

For the parameters used in Fig. 1 $S_m/ku^2 = 1/4$ formula (56) gives the amplitude $8\sqrt{2} = 11.3$ in reasonable agreement with the quasi-one-dimensional solution. The two-dimensional solution appears to have a more tightly bound nonlinear core than shown here.

The condition $k^2(u) > 0$ allows a wide range of vortex speeds u. The vortices considered most likely to be the nonlinear states evolved from the final stages of the fluid turbulence simulations are those with small u given by $u_{\min} = \pm(2\varepsilon_n K)^{1/2}$. These velocities scale with K and ε_n similar to the effective phase velocities $|\omega_k/k_y|$ of the fastest growing toroidal η_i-mode. From Eq. (56) the associated amplitude of the vortex structure is

$$\Phi_{\max} = c_\Phi \frac{2\varepsilon_n K}{|S_m|} \tag{57}$$

where c_Φ is a numerical constant. The scaling (57) is related to that of the mixing length estimate for wave turbulence $\gamma_k/|k_x|$ with $|k_x|$ replaced by magnetic shear and $\gamma_k/k_y \sim (2\varepsilon_n K)^{1/2}$ replaced by $2\varepsilon_n K$. Equation (57) should only be taken as an estimate of the scaling of the toroidal η_i-vortex structure amplitude. In fact, the simulations[6,7] suggest that the scaling with S_m is considerably weaker than $|S_m|^{-1}$.

V. Conclusions

Coherent vortex solutions associated with the nonlinear ion temperature-gradient perturbations are presented in detail including the effect of toroidicity and magnetic shear. We

show that the standard drift-wave vortex solutions can be generalized to the equations that include the ion temperature inhomogeneity, magnetic shear, shear flow, finite ion Larmor radius effects, and toroidicity effects.

Effects of shear introduce new scalar nonlinear terms in the equations for the electrostatic potential Φ. The case of relatively weak shear is studied in Sec. III. In the regime when the quadratic nonlinear terms given by Eq. (35) can be regarded as small, and higher nonlinear terms neglected, i.e. when the following inequality holds:

$$1 \gg \Phi \max\left(\frac{S_\perp}{u}\ ,\ \alpha\frac{S_m}{u^2\rho^2}\right) \gg \Phi^2\left(\frac{S_m}{u^2\rho}\right)^2 \tag{58}$$

we obtain a perturbed modon-type solution, Eqs. (32) and (37).

Although more general than the results of Ref. 3, our solution has a simpler structure, with a small amplitude monopole and quadrupole superimposed on the modon. Such dipole-like vortex structures are expected to be long-lived, and to develop as a result of a high level of fluctuations in the η_i turbulence. Similar coherent vortex solutions are found in the long time steady turbulent states produced in the numerical solutions of the fluid ion temperature-gradient driven turbulence.

A different type of solution is presented in Sec. IV for the case of relatively strong magnetic shear

$$\Phi_{\max}\left(S_m/u^2\rho\right) \sim 1\ . \tag{59}$$

An equation similar to a (real) cubic Schrödinger equation is obtained, with the main nonlinearity arising from the strong magnetic shear. A dipole vortex type solution of this equation is possible, if the fluctuation amplitude is large enough to produce wave trapping. Some features of this new type of vortex are studied numerically.

Acknowledgments

This work was initiated while one of the authors (D.J.) was visiting Risø National Laboratory, Denmark. The hospitality of the RNL institution is gratefully acknowledged. The numerical solutions were performed by D. Lindberg. The work is supported by the U.S. Department of Energy grant JF-944.

References

1. S. Hamaguchi and W. Horton, Plasma Phys. Contr. Fusion, **34**, 203 (1992).

2. B.G. Hong and W. Horton, Phys. Fluids B **2**, 978 (1990).

3. B.G. Hong, F. Romanelli, and M. Ottaviani, Phys. Fluids B **3**, 615 (1991).

4. H. Nordman and J. Weiland, Nuclear Fusion **29**, 251 (1989).

5. X-N. Su, W. Horton, and P.J. Morrison, Phys. Fluids B **4**, 1238 (1992).

6. W. Horton, R.D. Estes, and D. Biskamp, Plasma Phys. **22**, 663 (1980).

7. S. Hamaguchi and W. Horton, Phys. Fluids B **2**, 1833 (1990).

8. M. Ottaviani, F. Romanelli, R. Benzi, M. Briscolini, P. Santangelo, S. Succi, Phys. Fluids B **2**, 67 (1990).

9. B. Coppi, M.N. Rosenbluth, and R.Z. Sagdeev, Phys. Fluids **10**, 582 (1967).

10. W. Horton, D-I. Choi, and W.M. Tang, Phys. Fluids **24**, 1077 (1981).

11. P.K. Shukla, Physica Scripta **36**, 500 (1987).

12. P.K. Shukla and J. Weiland, Phys. Lett. A **136**, 59 (1989).

13. W. Horton, T. Tajima, and T. Kamimura, Phys. Fluids **30**, 3485 (1987).

14. T. Tajima, W. Horton, P.J. Morrison, J. Schutkeker, T. Kamimura, K. Mima, and Y. Abe, Phys. Fluids B **3**, 938 (1991).

15. S. Hamaguchi and W. Horton, Phys. Fluids B **4**, 319 (1992).

Figure Captions

1. The phase space $(\psi, d\psi/dx)$ trajectory of the solution of the cubic Schrödinger-like equation (53). The insert shows the small amplitude oscillations that occur in the exterior region. The dashed figure-eight curve is the separatrix from Eq. (55). The same solutions apply qualitatively for $|S_m| \approx |2\varepsilon_n + u(u-1)/(u+K)|/4$.

2. The nonlinear eigenfunction and the associated energy densities corresponding to Fig. 1 (a) The vortex eigenfunction with an enlargement of the tail region showing the small amplitude oscillations. (b) The energy densities of Φ^2, $(\nabla\Phi)^2$ and $\frac{1}{2}v^2$ computed from the solutions in (a).

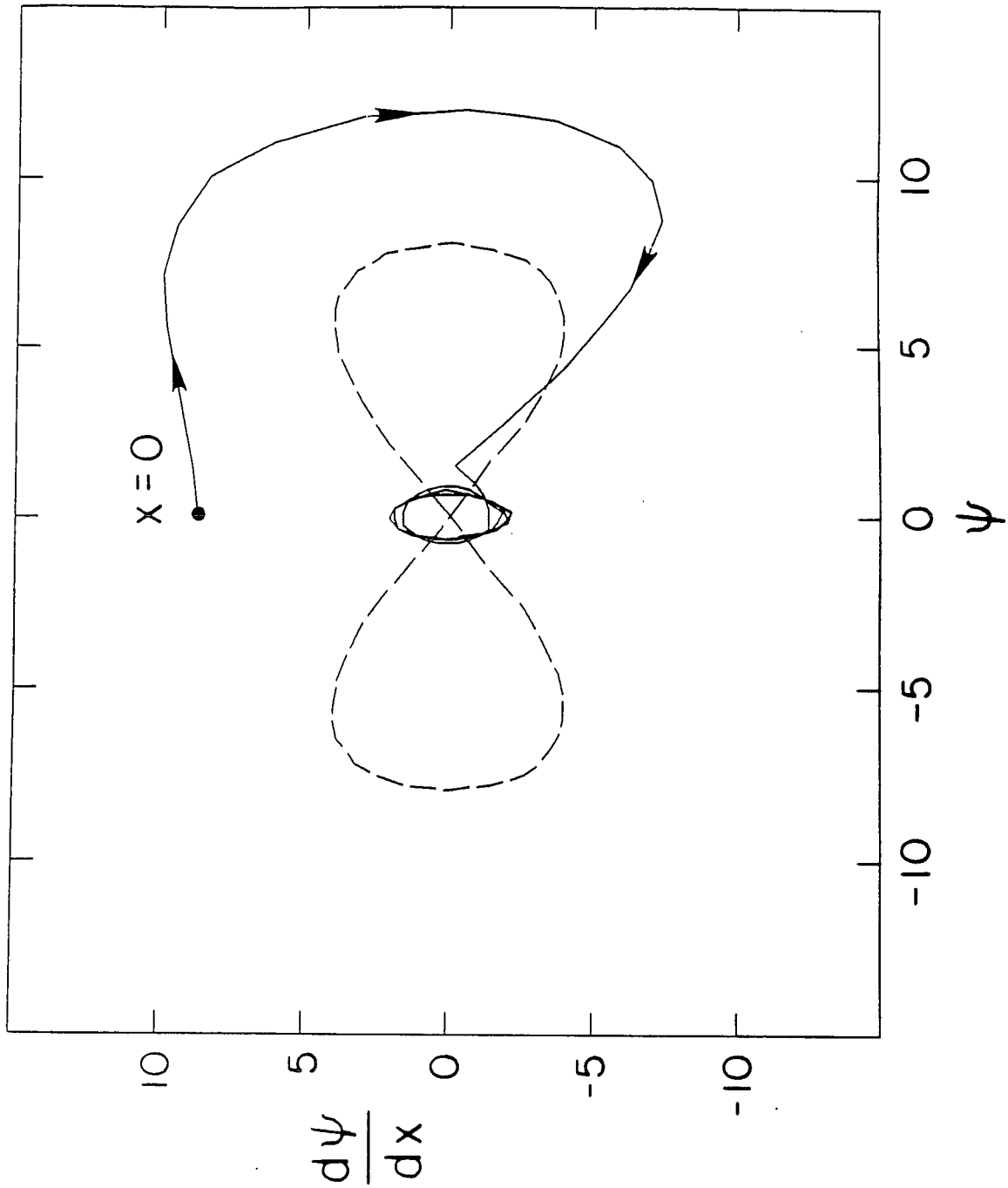

Fig. 1

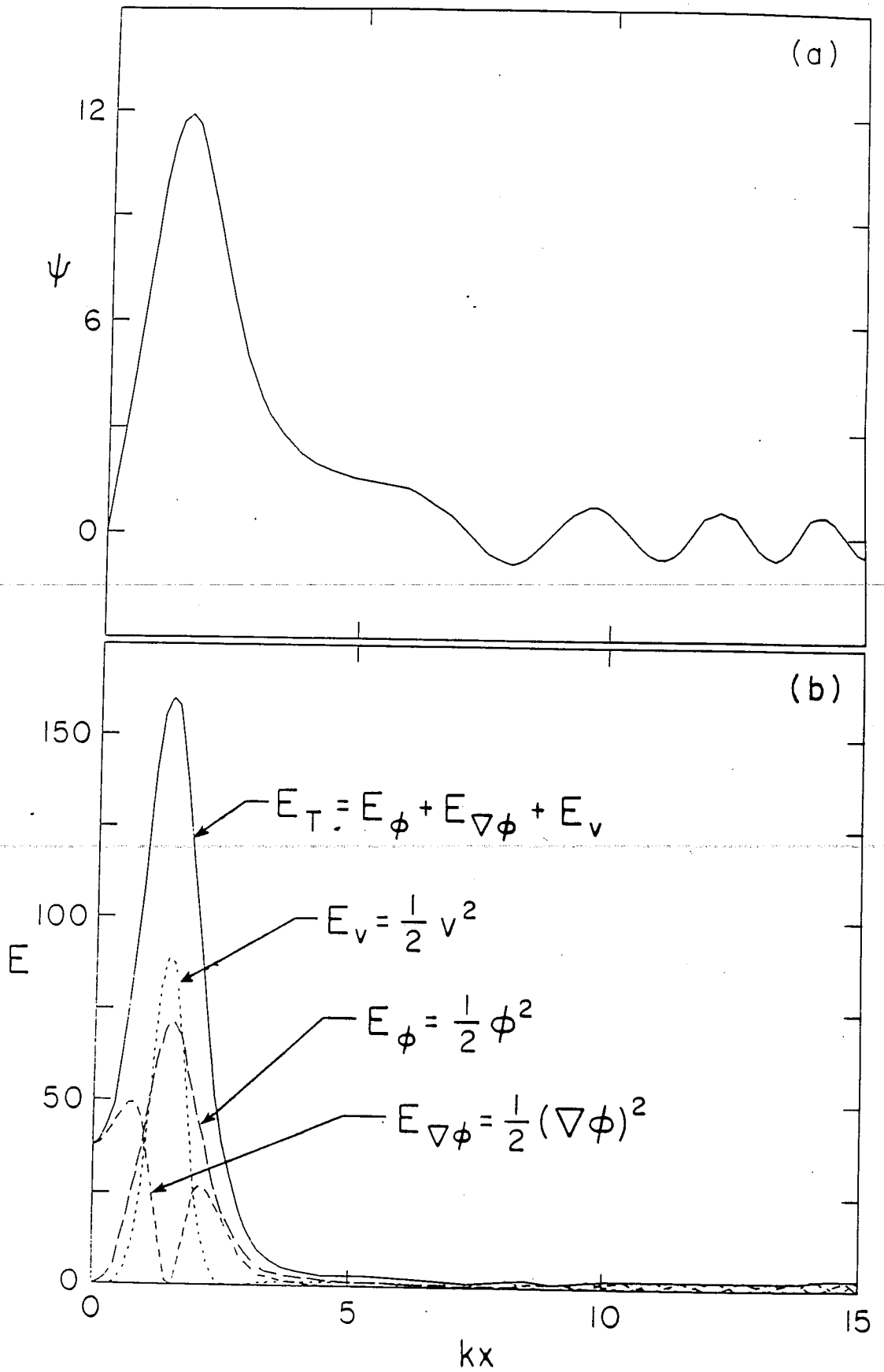
(a)
12
ψ
6
0
(b)
150
100
E
50
0
$E_T = E_\phi + E_{\nabla\phi} + E_v$
$E_v = \frac{1}{2} v^2$
$E_\phi = \frac{1}{2} \phi^2$
$E_{\nabla\phi} = \frac{1}{2} (\nabla\phi)^2$
0
5
10
15
kx

Fig. 2